Nanotechnology Perceptions
ISSN 1660-6795
www.nano-ntp.com

Photoinduced Antifungal and Thermal Studies of Functionally Modified Starch-Carbon Nanoparticle System

Sheena Varghese[1,2], Sunny Kuriakose[2]

[1]Department of Chemistry, Alphonsa college Pala, 686574, Mahatma Gandhi University, Kottayam, Kerala
[2]Research and Post Graduate Department of Chemistry, St. Thomas College, Pala – 686574, Mahatma Gandhi University, Kottayam, Kerala
Email: skresearchgroup@rediffmail.com

This paper aimed to explore the synthesis of carbon nanoparticle (CNP) from natural sources such as kitchen soot, synthesise of a chromophoric system {5-[4-(dimethylamino) benzylidene]-4-oxo-2-thioxo-1, 3-thiazolidin-3-yl} acetic acid and its incorporation into starch through DCC coupling, encapsulation of CNP in to scaffolds of functionally modified starch system, characterization of the products by UV-visible, FT-IR, 1HNMR, fluorescence spectroscopic methods, scanning electron microscopy (SEM), transmission electron microscopy (TEM) and X-ray diffraction (XRD) methods. It is also aimed to study the thermal stability, light fastening ability and photoinduced antifungal action of the products. The antifungal activity of functionally modified starch-CNP systems was tested against various pathogenic fungal strains such as Aspergillus niger, Aspergillus fumigates, Aspergillus flavus, Penicillium janthinellum, and Mucor ramosissimus by well method. The results showed that and functionally modified product have excellent photoinduced antifungal activity against selected fungal strains.

Keywords: Carbon nanoparticle, {5-[4-(dimethylamino) benzylidene]-4-oxo-2-thioxo1, 3-thiazolidin-3-yl} acetic acid, DCC coupling, starch, antifungal, Aspergillus niger, Aspergillus fumigates, Aspergillus flavus, Penicillium janthinellum, and Mucor ramosissimus.

1. Introduction

Nano materials have potential applications in biomedical nanotechnology. Nanoparticles can be used as antimicrobial agents because of its physical and chemical properties. Carbon nanoparticles exhibit significantly distinct physical, chemical and biological properties from their bulk counter parts because of small particle dimension, high surface area, quantum confinement and other effects. Carbon nanoparticles have different surface interactions compared to micron sized particles [1-3].

CNPs have an extremely high tendency of adhesion and aggregation. Surface coating of nanoparticles prevents degredation and protects the nanoparticles from aggregation and can help preserve different properties of the material [4-7]. Starch molecules which possess

scaffolds or channels are best suited for encapsulating nanoparticles. CNPs incorporated in to starch can enhance the solubility and bioavailability [8, 9]. The surface coating of carbon nanoparticles with starch enhances the biological applications such as antimicrobial activity.

Starch core is prone to functional transformation due to the presence of free hydroxyl functions in its backbone. Functionally modified, water-soluble, macromolecules like starch are expected to have very interesting photochemical properties which could provide applications in coating materials, printing, ink industries, dye industry, medical diagnosis and photodynamic therapy (PDT).

The present work gave thrust on the synthesis of CNPs from natural sources such as kitchen soot, functional modification of starch with the photoactive system {5-[4-(dimethylamino) benzylidene]-4-oxo-2-thioxo-1, 3-thiazolidin-3-yl} acetic acid and encapsulation of CNP in to the scaffolds of functionally modified starch aggregates [8]. We studied the antifungal activity of functionally modifided starch-CNP complex against selected fungal strains such as Aspergillus niger, Aspergillus fumigates, Aspergillus flavus, Penicillium janthinellum, and Mucor ramosissimus.

2. MATERIALS AND METHODS

The important chemicals, reagents and materials used for the work such as nitric acid, acetone, water, rhodanin-N-acetic acid, p-dimethyl amino benzaldehyde, β-naphthol, sodium hydroxide, dimethylformamide (DMF), hexane, ethyl acetate, chloroform, methanol, Agar Agar, starch and sodium nitrite and all the solvents were purchased from Merck (India). The solvents used for the study were purified by literature procedure. Dicyclohexyl carbodiimide (DCC) and dimethyl aminopyridine (DMAP) were purchased from Aldrich and M.H.Agar from 'The Institute of Microbial Technology (IMTECH) Chandigarh, India'. The surface morphology and the internal structure were probed with a HITACHI S-4200 scanning electron microscope (SEM) operated at 10KV. Infrared spectra in the range 400-4000cm^{-1} were recorded at 64 scans per spectrum at 2cm^{-1} resolution using Shimadzu IR 470 FTIR spectrophotometer. ^{1}H-NMR spectra were recorded on a Bruker DRX 500 FT-NMR spectrophotometer at 400 MHz. UV-visible spectra were recorded on a Shimadzu UV-visible spectrophotometer using the operating wavelength in the range 190-1100 nm. Fluorescence spectra were recorded on a Perkin Elmer LS 45 fluorescence spectrometer.

(i) Synthesis of carbon nanoparticles by chemical methods

Carbon nanoparticles were synthesised by refluxing the purified kitchen soot in nitric acid. Typically 2g of soot was refluxed in 200ml of 5M nitric acid at 100^{0}C for 6 hr and cooled down to room temperature. The brownish yellow supernatant liquid was neutralized by sodium carbonate. The excess solvent was removed on a vacuum rotary flash evaporator at reduced temperature and carbon nanoparticles were separated from the solution by centrifugation. The samples may contain impurities and it was dissolved in acetone-water (3:1) mixture. The undissolved residue was discarded after filtration. The clear solution was collected and the solvent was evaporated off on a vacuum rotary evaporator [8].

(ii) Synthesis of {5-[4-(dimethylamino) benzylidene]-4-oxo-2-thioxo-1, 3-thiazolidin-3-yl} acetic acid

P-dimethylaminobenzaldehyde (1g) and rhodanin-N-acetic acid (1.25g) were dissolved in ethanol (50 ml). The mixture was stirred thoroughly for a few minutes. The temperature was raised to 80^0C and the mixture was refluxed for 4 hours. The product was filtered. It was purified by recrystallisation from absolute ethanol. The yield was noted as 80% (Chandran et al. 2012). It was further purified by column chromatography using (10:3) hexane-ethyl acetate solvent systems and dried in vacuum [8,19].

(iii) Synthesis of starch functionalised with {5-[4-(dimethylamino) benzylidene]-4-oxo-2-thioxo-1, 3-thiazolidin-3-yl} acetic acid

Starch and the dye in molar ratio (1g), DMAP (200 mg), and DCC (1 g) were separately dissolved in DMF and introduced into an R.B flask fitted with a reflux condenser and a magnetic stirrer cum heater. The mixture was stirred at room temperature for 2 hours and at 80^0C for 6 hours. The by-product dicyclohexyl urea (DCU) was removed by warming-cooling-filtration processes and the solvent was removed in a vacuum rotary evaporator and dried. The product was purified by column chromatography using chloroform-methanol and dried in vacuum.

(iv) Encapsulation of CNP in the scaffolds of starch functionalised with {5-[4-(dimethylamino) benzylidene]-4-oxo-2-thioxo-1, 3-thiazolidin-3-yl} acetic acid

Carbon nanoparticles were dissolved in chloroform (20 ml) and were added to starch functionalised with {5-[4-(dimethylamino) benzylidene]-4-oxo-2-thioxo-1, 3-thiazolidin-3-yl} acetic acid in water (20 ml). The reaction mixture was stirred at room temperature for 6 hours. The encapsulated products in the aqueous layer were separated from the chloroform layer and solvents were removed in a vacuum rotary evaporator, dried and kept under vacuum.

(v) Thermal studies

Thermal analysis of CNP, starch, photochromic system, functionally modified starch, and functionalised starch-CNP samples was carried out on a TA instrument, SDT Q600. Around 30mg of the sample was taken in an alumina pan. The experiment was carried out in air atmosphere from ambient to 800^0C and ramp rate was kept at 10^0per minute. TA universal analysis software was used for data interpretation [8].

(vi) Light fastening studies

{5-[4-(dimethylamino) benzylidene]-4-oxo-2-thioxo-1, 3-thiazolidin-3-yl} acetic acid (dye), starch-dye, and starch-dye- CNP were subjected to irradiation with visible light for a period of zero to four hours. The spectral measurements were carried out with solutions of same molar concentrations (0.2mg/ml) in chloroform. The changes in the absorption spectra as a function of time were noted.

(vii) Photoinduced antifungal study

The Agar well-diffusion method was used to test the antifungal activity. For in vitro screening, fungi, such as Aspergillus niger, Aspergillus fumigates, Aspergillus flavus, Penicillium janthinellum, and Mucor ramosissimus were selected. The photoinduced antifungal effects of functionally modified starch-CNP systems were tested with the above five pathogenic fungal strains. In this study the sample was irradiated with visible light for 0.5 hr, 1 hr, 2 hrs and 4 hrs durations. Samples of the irradiated system were immediately withdrawn and the activity

studies were conducted. Using sterile micro pipette 200µlts of the sample solutions (irradiated and nonirradiated) were poured into each well. Three replications and control tests were conducted. Controls used for the measurement were water, dye, starch and starch-dye. After incubation times (96 hrs) the zones of inhibition (in mm) were measured [20, 21, 23]. MIC of the samples was examined by a micro dilution method. 200µl solutions of fraction of samples (100µg/ml, 200µg/ml, 300µg/ml and 400µg/ml) were added in the well in the lawned plate. All the plates were incubated at 30-35ºC for 24-96 hours. The lowest concentrations that would inhibit the growth of fungal strain were taken as MIC [20].

3. RESULTS AND DISCUSSION

(i) Synthesis and characterisation of carbon nanoparticles

CNPs were synthesized from kitchen soot by thermal refluxion with nitric acid. The solubility of the carbon nanoparticles powder was tested with different solvents and found to be soluble in methanol, chloroform, acetone, DMF, water and (3:1) acetone-water mixture. The good solvent systems for CNP were taken as (3:1) acetone-water mixture, water and chloroform (table 1). Figure 1 represents carbon nanoparticles (powder) and different (5mg/ml) CNPs solutions.

Table 1. Solubility of carbon nanoparticles

SI. No	Solvents	Solubility*
1	(3:1) Acetone-water mixture	≤95%
2	Chloroform	≤90%
3	Water	≤90%
4	Methanol	≥82%
5	Acetone	≥62%
6	DMF	≥60%
7	Hexane	≥5%
8	Tolune	≥5%

* highly soluble (90-100%), soluble (50-90%), less soluble (10-50%), not soluble (below 10%)

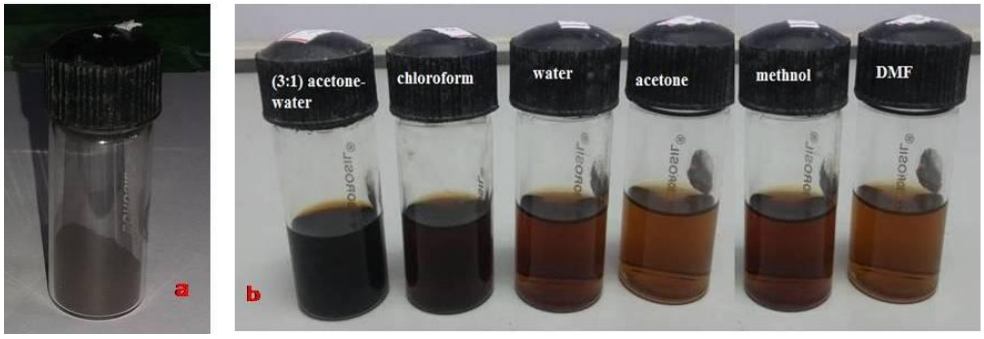

Figure 1. Photographs of (a) powder form of CNPs and (b) different (5mg/ml) CNPs solutions.

The carbon nanoparticles were characterized by UV/visible spectroscopy, fluorescence spectroscopy, SEM, TEM and XRD. The UV/visible absorption and fluorescence

emission spectra of CNP were recorded in chloroform. The absorption maximum (λmax) of CNP was obtained at 412 nm. This is due to the $\pi - \pi^*$ transitions. The fluorescence emission maximum for CNP was observed at 433nm. Figure 2(a) and 2(b) shows the UV-visible absorption and fluorescence emission spectra of carbon nanoparticles respectively. Figure 3(a) and 3(b) shows the photographs of 1 mg/ml (3:1) acetone-water solution of carbon nanoparticles in normal visible light and on exposure to UV light respectively. Fluorescence carbon nanoparticles with particle size 10 ±5 nm showed greenish blue emission when exposed with UV light [22].

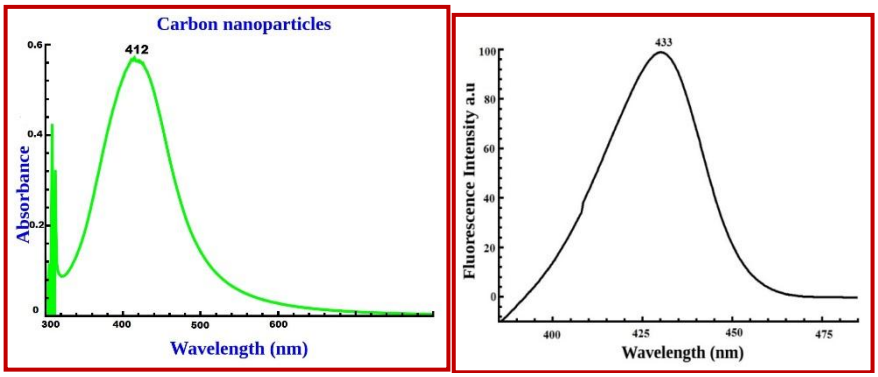

(a) (b)

Figure 2. (a) UV-visible absorption and (b) fluorescence emission spectra of carbon nanoparticles

(a) (b)

Figure 3. Photographs of 1 mg/ml (3:1) acetone-water solution of carbon nanoparticles (a) in normal visible light and (b) exposed to UV light

SEM was used for surface analysis of the CNP in order to investigate the morphology of the particles. The SEM image shows almost uniform particle size and distribution of particles. The TEM image shows particle size in the range 2-20nm. XRD was used as a method

of determining the arrangement of atoms within a crystal and also the size of the carbon nanoparticle. The results are shown in figure 4.

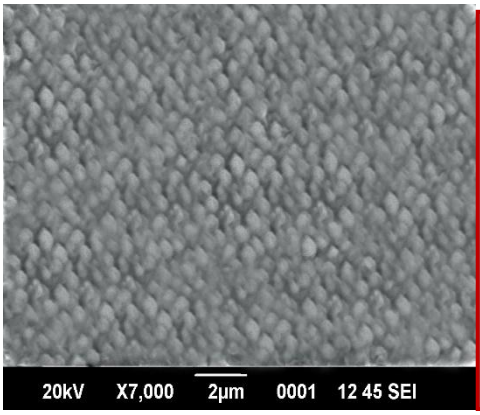

(a)

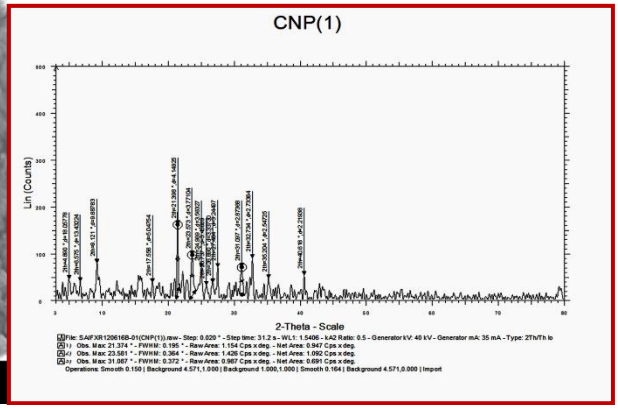

(b)

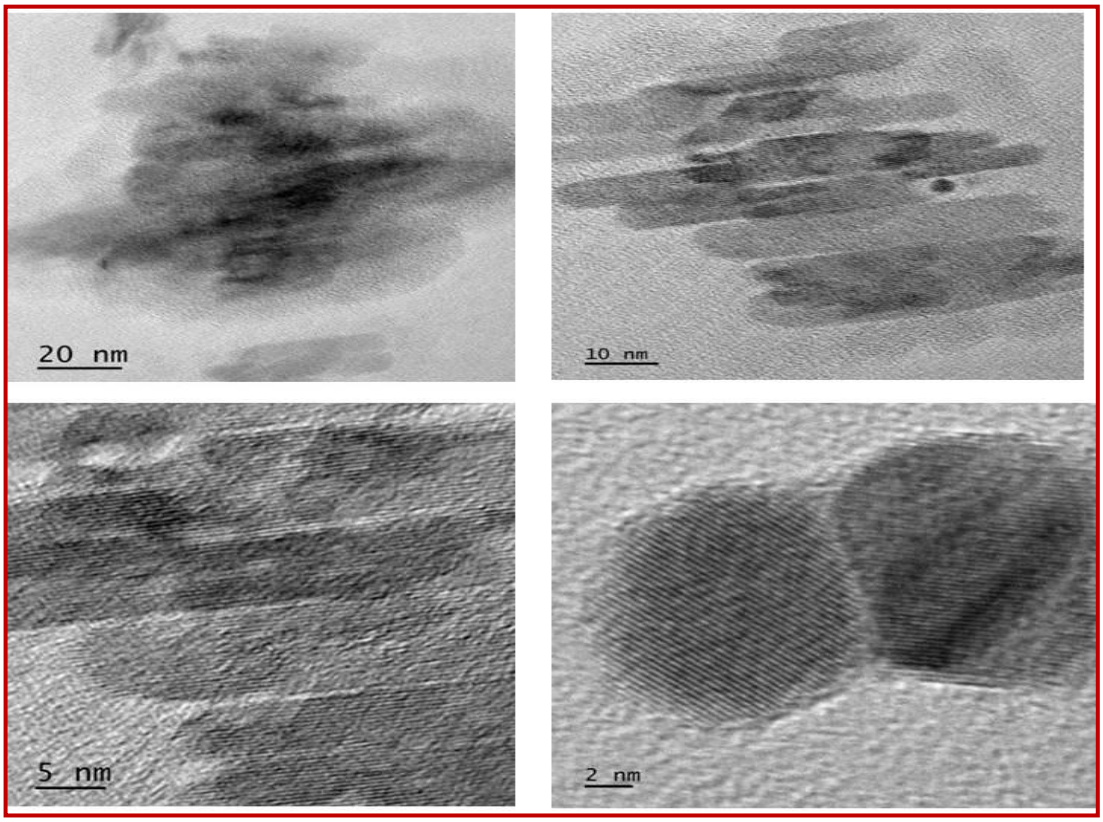

(c)

Figure 4. (a) SEM image (b) XRD pattern and (c) TEM image of carbon nanoparticle

(ii). Synthesis and characterisation of {5-[4-(dimethylamino) benzylidene]-4-oxo-2-thioxo-1,

3-thiazolidin-3-yl} acetic acid

The photoactive {5-[4-(dimethylamino) benzylidene]-4-oxo-2-thioxo-1, 3-thiazolidin-3-yl} acetic acid was prepared from p-dimethylaminobenzaldehyde and rhodanin-N-acetic acid (scheme 1). The product was characterized by UV-visible, FT-IR, ^{1}HNMR and fluorescence spectroscopic studies.

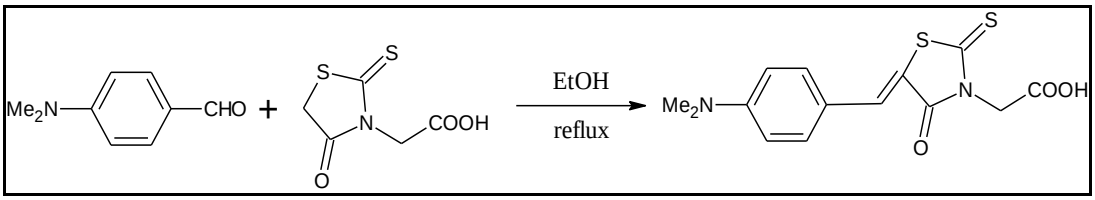

Scheme 1. Synthesis of {5-[4-(dimethylamino) benzylidene]-4-oxo-2-thioxo-1, 3-thiazolidin-3-yl} acetic acid

The UV-visible absorption and fluorescence emission spectra of {5-[4-(dimethylamino) benzylidene]-4-oxo-2-thioxo-1,3-thiazolidin-3-yl} acetic acid were recorded in chloroform. The absorption maximum (λ_{max}) of the dye was obtained at 464.5 nm. This is due to the n-π^* transition of the conjugated carbonyl group present in the chromophoric system. The fluorescence emission maximum for the chromophoric system was observed at 507 nm. Figure 5 presents the UV-visible absorption and fluorescence emission spectra of {5-[4-(dimethylamino) benzylidene]-4-oxo-2-thioxo-1, 3-thiazolidin-3-yl} acetic acid.

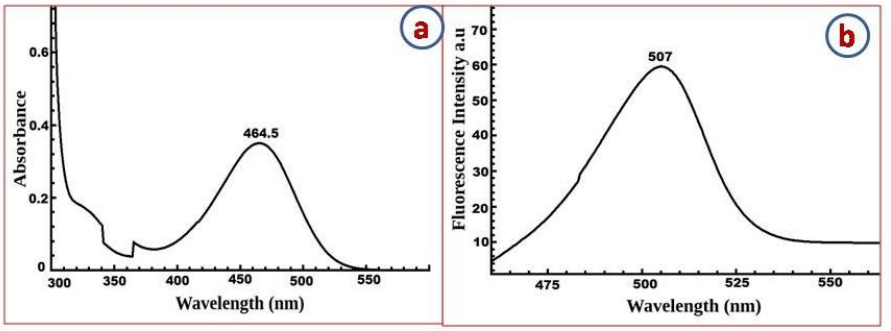

Figure 5. (a) UV-visible absorption and (b) fluorescence emission spectra of {5-[4-(dimethylamino) benzylidene]-4-oxo-2-thioxo1, 3-thiazolidin-3-yl} acetic acid

FT-IR spectrum of {5-[4-(dimethylamino)benzylidene]-4-oxo-2-thioxo-1,3-thiazolidin-3-yl} acetic acid was recorded in the solid state as KBr discs in the operating frequency range 4000–400cm^{-1} (figure 6). IR (KBr) : 3300-3500 cm^{-1}(broad): ν_{O-H} (str), 2922 cm^{-1}: ν_{C-H} of CH_2, 1714 cm^{-1}: $\nu_{C=O}$(str) , 1562 cm^{-1}: $\nu_{C=C}$(str), 1519 cm^{-1}: ν_{C-S} (str), 1315 cm^{-1}: ν_{C-N} (str), 1244 cm^{-1}: $\nu_{C=S}$ (str), 1103 cm^{-1}: ν_{C-O} (str).

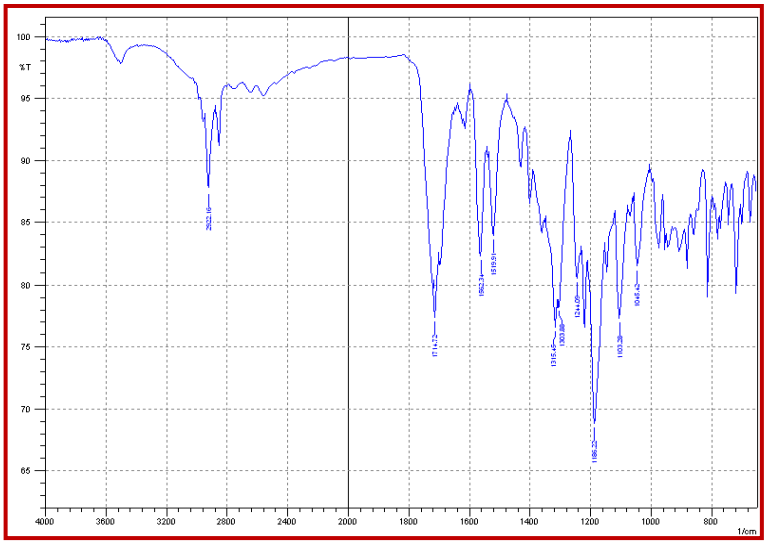

Figure 6. FT-IR spectrum of {5-[4-(dimethylamino) benzylidene]-4-oxo-2-thioxo-1, 3-thiazolidin-3-yl} acetic acid

^{1}HNMR spectrum of {5-[4-(dimethylamino) benzylidene]-4-oxo-2-thioxo1, 3-thiazolidin-3-yl} acetic acid was recorded in a 400 MHz instrument using $CDCl_3$ as solvent (figure 7). The molecule has 6 sets of chemically different protons which give six NMR signals. ^{1}H-NMR: 10.372 ppm (-COOH, H, s), 7.780 ppm (Ha, 2H, d), 6.747 ppm (Hb, 2H, d), 7.317 ppm (Hc, 1H, s) and 4.817 ppm (Hd, 2H, s) and 3.117 ppm (NMe_2, 6H, s).

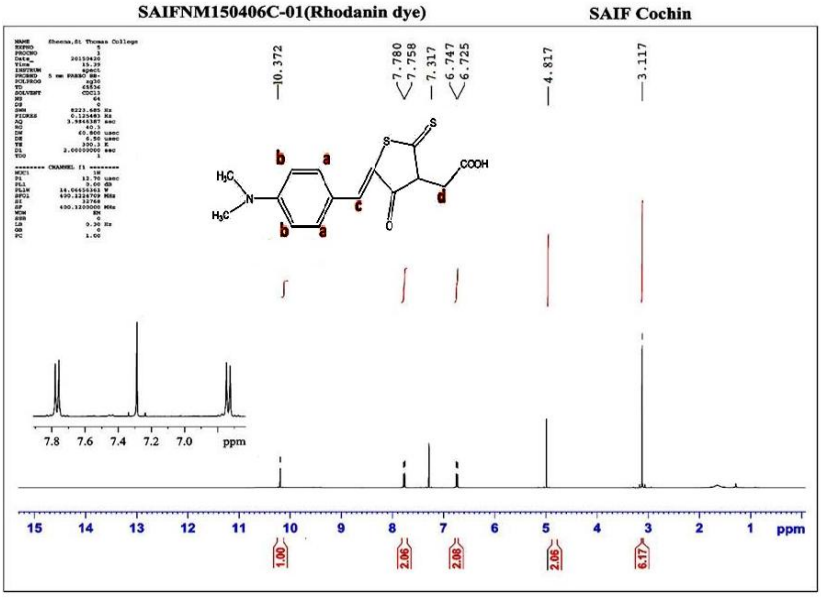

Figure 7. ^{1}HNMR spectrum of {5-[4-(dimethylamino) benzylidene]-4-oxo-2-thioxo-1, 3-thiazolidin-3-yl} acetic acid

(iii) Synthesis and characterisation of starch functionalised with {5-[4- (dimethylamino) benzylidene]-4-oxo-2-thioxo1, 3-thiazolidin-3-yl} acetic acid

The hydroxyl groups of starch were esterified with the free carboxyl group of {5-[4-(dimethylamino) benzylidene]-4-oxo-2-thioxo-1, 3-thiazolidin-3-yl} acetic acid through DCC coupling using DMAP as the catalyst (scheme 2). The products were characterized by UV-visible, FT-IR, ^{1}HNMR and fluorescence spectroscopic methods.

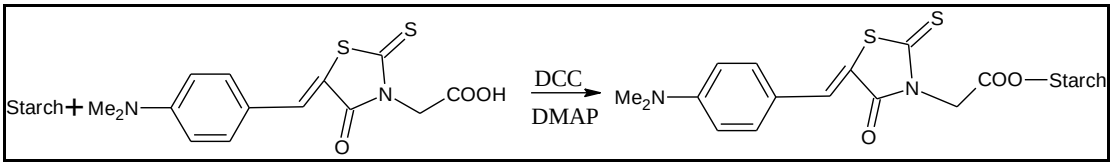

Scheme 2. Functional modification of starch with {5-[4-(dimethylamino) benzylidene]-4-oxo-2-thioxo-1, 3-thiazolidin-3-yl} acetic acid

The UV-visible absorption and fluorescence emission spectra of starch functionalized with {5-[4-(dimethylamino) benzylidene]-4-oxo-2-thioxo-1, 3-thiazolidin-3-yl} acetic acid was recorded in chloroform (figure 8). The λ_{max} of the original dye was obtained at 464.5 nm and the signal was shifted to 492 nm on attaching to starch. The peak at 492 nm is due to n-π^* transition of the starch supported by chromophoric system. The fluorescence emission maximum of 507 nm of {5-[4-(dimethylamino) benzylidene]-4-oxo-2-thioxo-1, 3-thiazolidin-3-yl} acetic acid was shifted to 534 nm in functionalised starch system which showed a red shift of 27 nm. Photochromic group is attached to core group such as starch and the energy gap between the molecular orbitals is reduced and hence the absorption and emission maxima get enhanced.

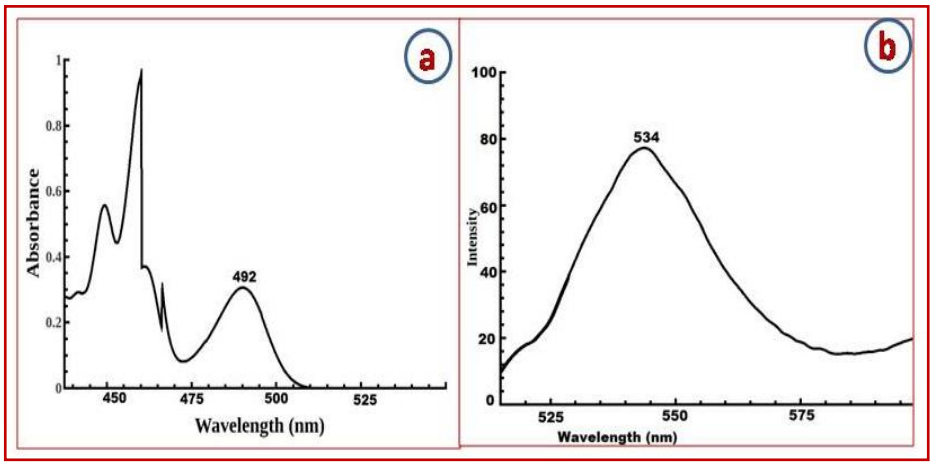

Figure 8. (a) UV-visible absorption and (b) fluorescence emission spectra of starch functionalised with {5-[4-(dimethylamino) benzylidene]-4-oxo-2-thioxo-1, 3-thiazolidin-3-yl} acetic acid

FT-IR spectra of starch and functionally modified starch were recorded in the solid state as KBr discs in the operating frequency range 4000–650 cm^{-1} (figure 9). IR (KBr) of starch: 3300 cm^{-1}(broad): ν_{O-H}(str), 2905 cm^{-1}: ν_{C-H} of CH_2, 1716 cm^{-1}: FT-IR (KBr) of functionally

modified starch: 3323 cm^{-1}(broad): ν_{O-H}(str), 2927 cm^{-1}: ν_{C-H} of CH_2, 1729 cm^{-1}: $\nu_{C=O}$(str), 1606cm^{-1}: $\nu_{C=C}$(str), 1323 cm^{-1}: ν_{C-O}(str), 1288 cm^{-1}: ν_{C-N}(str), 1105 cm^{-1}: $\nu_{C=S}$(str), 1082 cm^{-1}: ν_{C-S}(str).

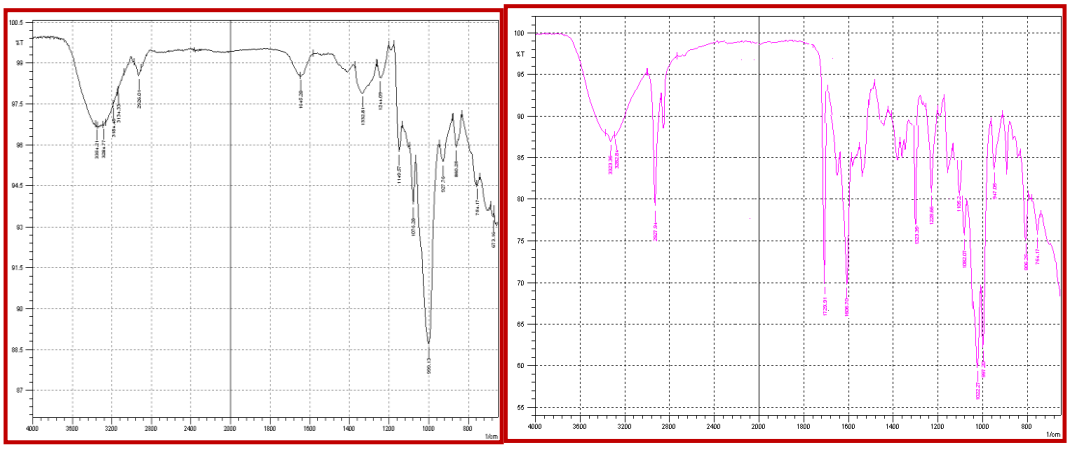

(a) (b)

Figure 9. IR spectra of (a) pure starch and (b) starch functionalised with {5-[4-(dimethylamino) benzylidene]-4-oxo-2-thioxo-1, 3-thiazolidin-3-yl} acetic acid

^{1}HNMR spectrum of the product was recorded in a 400 MHz instrument using $CDCl_3$ as solvent (figure 10). The results are: 7.756 ppm (Ha, 2H, d), 6.608 ppm (Hb, 2H, d) 7.285 ppm (Hc, 1H, s), 4.756 ppm (Hd, 2H, s), and 3.092 ppm (NMe_2, 6H, s), 2.903-1.100 ppm (H of starch, m). The COOH proton gave a signal at 9-11 ppm in the dye and this was absent in the coupled product due to complete esterification of the carboxylic group.

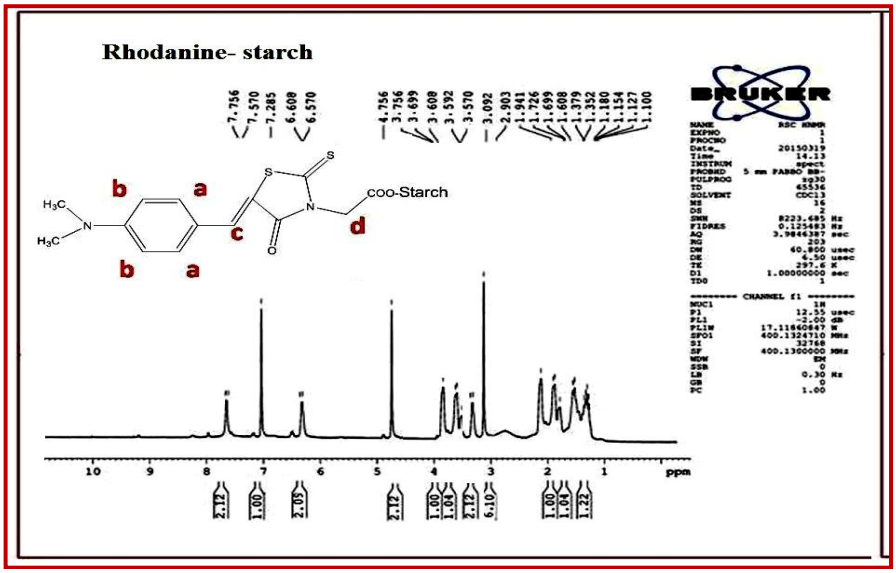

Figure 10. ^{1}HNMR spectrum of starch functionalised with {5-[4-(dimethylamino) benzylidene]-4-oxo-2-thioxo-1, 3-thiazolidin-3-yl} acetic acid

(iv) Synthesis and characterisation of CNP encapsulated in the scaffolds of starch functionalised with {5-[4-(dimethylamino) benzylidene]-4-oxo-2-thioxo-1, 3-thiazolidin-3-yl} acetic acid

CNPs were dissolved in chloroform and mixed with starch functionalised with {5-[4-(dimethylamino) benzylidene]-4-oxo-2-thioxo-1, 3-thiazolidin-3-yl} acetic acid in water (scheme 3). The product was characterised by UV-visible, fluorescence emission, ^{1}HNMR and FT-IR spectroscopic methods.

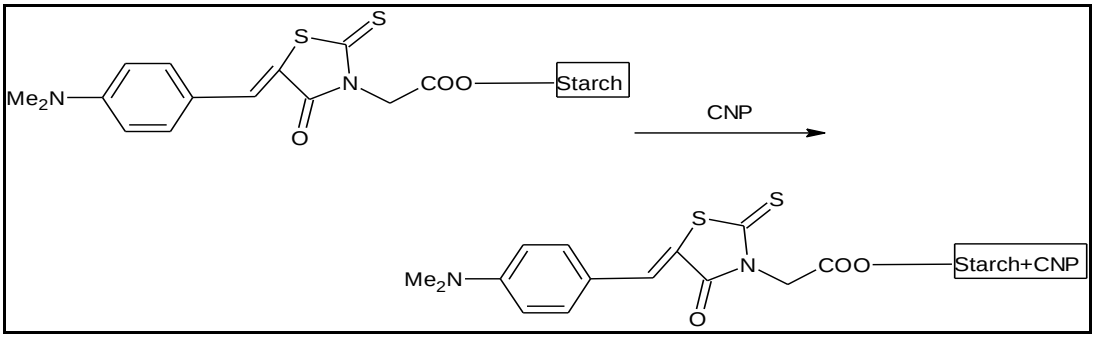

Scheme 3. Encapsulation of CNPs in starch functionalised with {5-[4-(dimethylamino) benzylidene]-4-oxo-2-thioxo-1,3-thiazolidin-3-yl} acetic acid

The UV-visible absorption and fluorescence emission spectra of CNP encapsulated in the scaffolds of starch functionalised with {5-[4-(dimethylamino) benzylidene]-4-oxo-2-thioxo-1, 3-thiazolidin-3-yl} acetic acid was recorded in chloroform (figure 11). The λ_{max} of the dye was shifted from 464.5 nm to 514 nm in functionalized starch-CNP system which showed a remarkable red shift of 49.5 nm. The fluorescence emission maximum of 507 nm of {5-[4-(dimethylamino) benzylidene]-4-oxo-2-thioxo-1, 3-thiazolidin-3-yl} acetic acid (dye) was shifted to 568 nm in functionalised starch-CNPs complex. This is equivalent to a red shift of 61 nm. The fluorescence emission wavelength and intensity were greatly enhanced on attaching CNP to the functionalised starch-chromophore system.

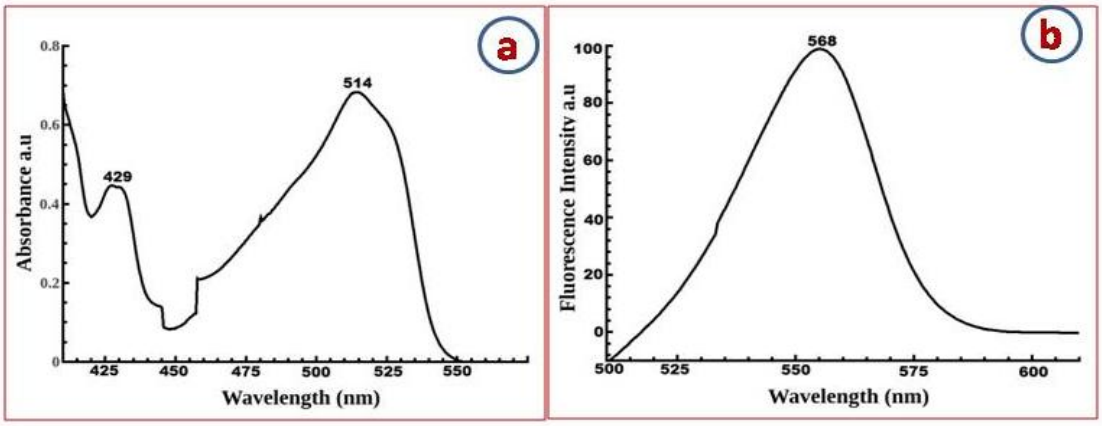

Figure 11. (a) UV-visible absorption and (b) fluorescence emission spectra of CNPs

encapsulated in the scaffolds of starch functionalised with {5-[4-(dimethylamino) benzylidene]-4-oxo-2-thioxo1,3-thiazolidin-3-yl} acetic acid.

FT-IR spectrum of CNP-starch-dye was recorded in the solid state as KBr discs in the operating frequency range 4000–650 cm^{-1} (figure 12). IR(KBr): 3328 cm^{-1}(broad): ν_{O-H} (str), 2927 cm^{-1}: ν_{C-H} of CH_2, 1727 cm^{-1}: $\nu_{C=O}$(str) , 1235 cm^{-1}: $\nu_{C=C}$(str) , 1388 cm^{-1}: ν_{C-N} (str), 1040 cm^{-1}: ν_{C-O} (str), 806 cm^{-1}: ν_{C-S}(str).

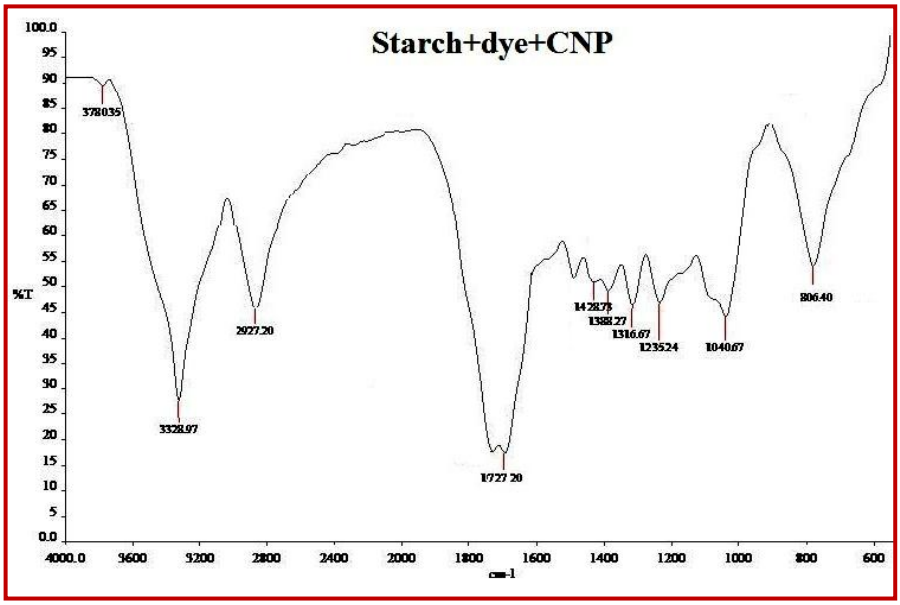

Figure 12. FT-IR spectrum of CNP in the scaffolds of starch functionalised {5-[4-(dimethylamino) benzyliden]-4-oxo-2-thioxo-1, 3-thiazolidin-3-yl} acetic acid.

^{1}HNMR spectrum of the product was recorded in a 400 MHz instrument using $CDCl_3$ as solvent (figure 13). The results are: 7.756 ppm (Ha, 2H, d), 6.528 ppm (Hb, 2H, d) 7.284 ppm (Hc, 1H, s), 5.031 ppm (Hd, 2H, s), and 3.107 ppm (NMe_2, 6H, s), 1.945-1.287 ppm (H of starch, m). The absence of a peak at 9-11ppm shows that the carboxylic proton is absent in the product and this shows the coupling of free carboxylic group of the dye with hydroxyl function of starch.

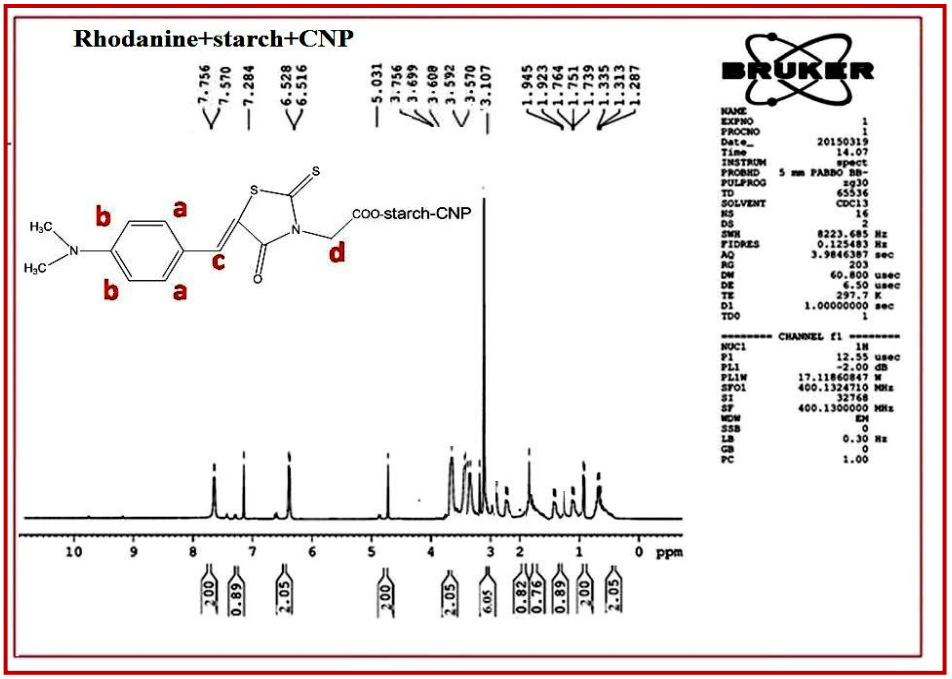

Figure 13. ^{1}HNMR spectrum of CNP in the scaffolds of starch functionalised {5-[4-(dimethylamino) benzyliden]-4-oxo-2-thioxo-1, 3-thiazolidin-3-yl} acetic acid

(v) Thermal studies

Thermal analysis gives information about changes in material properties as a function of temperature. A comprehensive study of a materials thermal behaviour is possible by TGA and DSC which measures changes in weight in relation to changes in temperature. The measured weight loss curve gives information on changes in sample composition and thermal stability of the sample. A derivative weight loss curve can be used to tell the point at which weight loss is most apparent. On comparing the results of thermal analysis of different samples of CNP, starch, photochromic system, functionally modified starch, and modified starch-CNP the greater thermal stability was found in functionally modified starch-CNP. The complete thermal decomposition of CNPs and functionally modified starch-CNP was achieved at 460°C and 520°C respectively. On comparing the results of thermal analysis of different samples such as CNP, {5-[4-(dimethylamino) benzylidene]-4-oxo-2-thioxo-1, 3-thiazolidin-3-yl} acetic acid (dye), starch, starch-dye and starch-dye-CNP, the maximum thermal stability (≥520°C) was found for starch-dye-CNP system. The greater thermal stability of functionally modified starch-CNP is due to the strong intraction of starch core and CNP. The results of the TGA-DSC analysis are shown in table 2 and figure 14.

Table 2. Thermal analysis results

Systems	Temperature	Peak temperature	Thermal stability (complete decomposition)	Mass loss
CNP	50^{0}C-130^{0}C	100^{0}C		18.72%
	200^{0}C-460^{0}C	410^{0}C	$\geq 460^{0}$C	56.85 %
starch	20^{0}C-100^{0}C	80^{0}C		22.72%

	250^{0}C-330^{0}C	300^{0}C	$\geq 330^{0}$C	66.85 %
Dye	50^{0}C-110^{0}C	88^{0}C		10.50%
	125^{0}C-300^{0}C	230^{0}C	$\geq 300^{0}$C	82.00 %
Dye+starch	20°C-90°C	75^{0}C		10.55%
	200°C-400°C	280°C, 350°C	≥400°C	86.69%
Starch+dye+CNP	30°C-100°C	80°C		12.55%
	100°C-300°C	210°C		72.86%
	400°C-520°C	460°C	≥520°C	16.25%

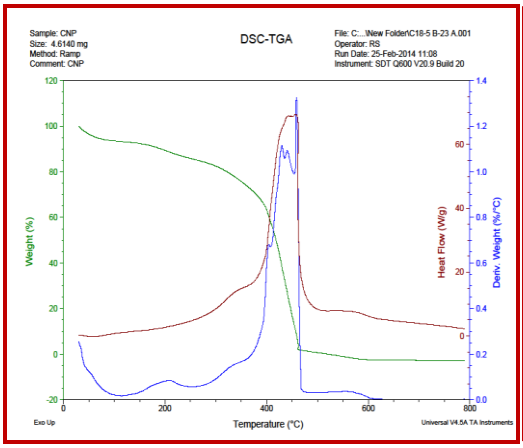

(a)

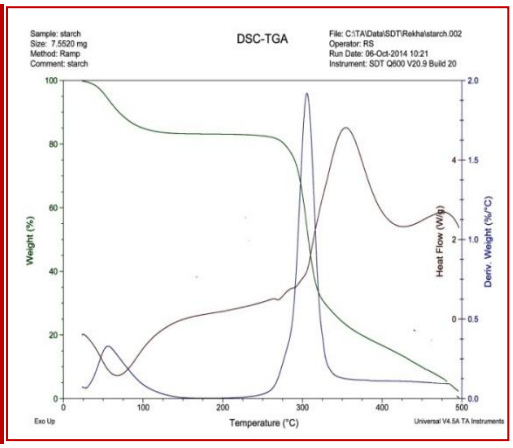

(b)

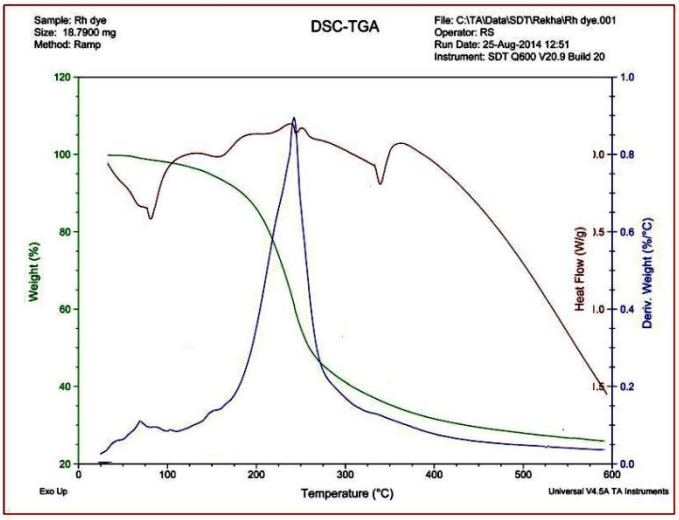

(c)

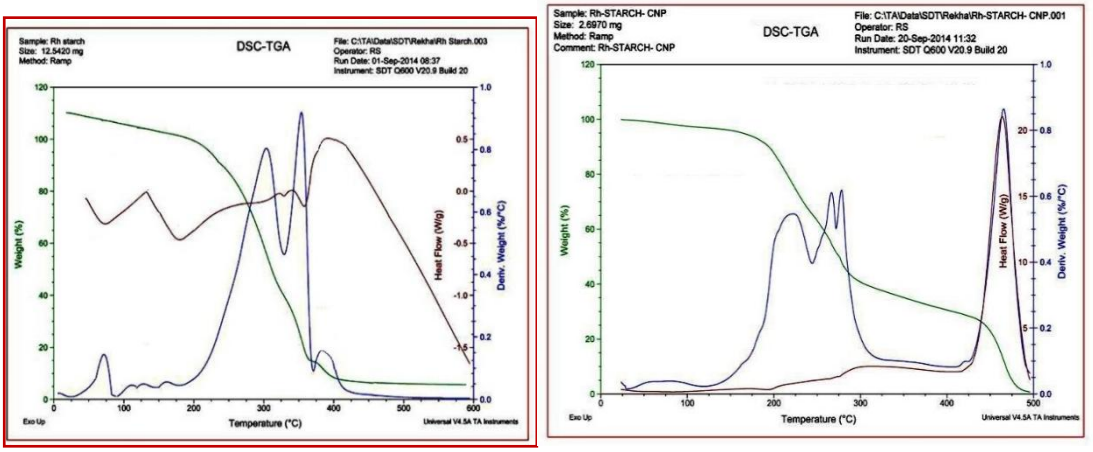

(d) (e)

Figure 14. TGA-DSC of (a) carbon nanoparticles (b) starch (c) dye (d) functionally modified starch (e) functionally modified starch-CNP system

(vi) Light fastening studies

{5-[4-(dimethylamino) benzylidene]-4-oxo-2-thioxo-1, 3-thiazolidin-3-yl} acetic acid (dye), starch-dye, and starch-dye- CNP were subjected to irradiation with visible light for a period of zero, half, one, two and four hours. Results showed that for {5-[4-(dimethylamino) benzylidene]-4-oxo-2-thioxo-1, 3-thiazolidin-3-yl} acetic acid, a signal was obtained at 464.5nm and this signal showed a decrease in intensity of absorption on irradiation with visible light. The intensity of absorption was 0.612 a.u. at zero time. After one hour irradiation, the intensity was reduced to 0.398 a.u and after four hours irradiation, remarkable decrease in intensity was noted (0.097 a.u). Starch-dye systems showed absorption maxima at 492 nm with intensity of absorption 0.608 a.u at zero time of irradiation and the intensities were reduced to 0.526 a.u after one hour of irradiation. On irradiation for four hours there was no further decrease in the absorption intensity of starch-dye systems. The dye showed noticeable stability and light fastening on attaching to starch core systems. This indicates that the functionally modified starch can show remarkable stability on irradiation.

For the functionally modified starch-CNP systems, there was no change in the intensity of absorption on irradiation with visible light for a period of four hours. The intensity of absorption was noted as 0.472 a.u at zero time, which remains almost intact on irradiation for 4 hours. Strong red shifts were observed on binding the chromophore to core systems and on encapping CNPs in starch systems. The results showed that the stability of functionally modified core-CNP systems was greatly enhanced and provides a new and novel photosensitive system with excellent light fastening properties. The results are summarized in table 3 and figure 15.

Table 3. Light stabilization studies on photoresponsive systems (comparison of $\lambda_{max,}$ red shift and intensity of absorption)

Systems	λ_{max} (nm)	Red shift in comparison with dye (nm)	Intensity of absorption (atomic units-a.u) (Time interval for light irradiation)				
			Zero hr	0.5 hr	1 hr	2 hrs	4 hrs
Dye	464.5	-	0.612	0.451	0.398	0.215	0.097
Dye+starch	492	29.5	0.608	0.526	0.526	0.526	0.526
Starch+Dye+CNP	514	49.5	0.472	0.472	0.472	0.472	0.472

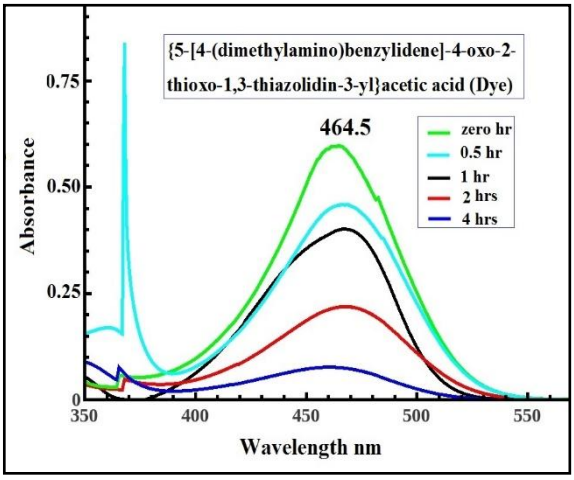

(a)

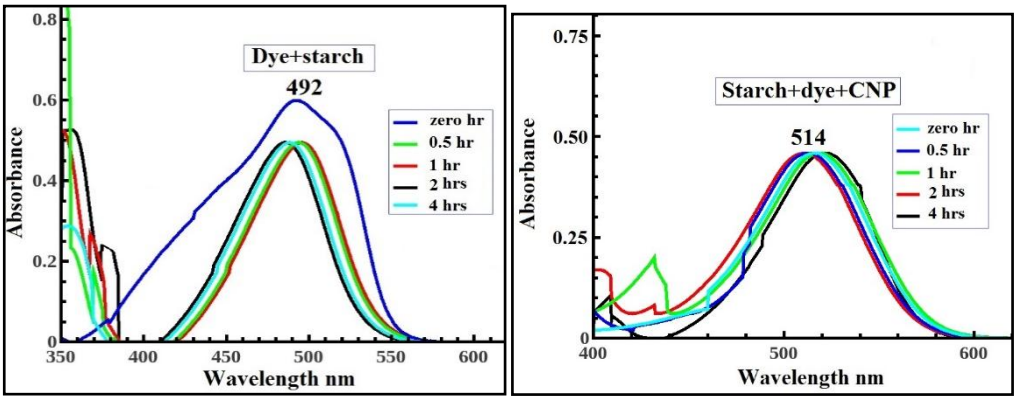

(b) (c)

Figure 15. Light stabilization studies on photoresponsive systems (a) dye (b) starch-dye (c) starch-dye-CNP

(vii) Photoinduced antifungal activity of functionalised starch-CNP system

(a) Minimum inhibitory concentration (MIC) of functionalised starch-CNP system

The minimum inhibitory concentrations (MIC) were examined by a micro dilution method. 200µl solutions of fraction of samples (100µg/ml, 200µg/ml, 300µg/ml, 400µg/ml and 500µg/ml) were added in the well in the lawned plate. All the plates were incubated at 28°C

for 96 hrs. The lowest concentrations that would inhibit the growth of fungal strains were taken as MIC. MIC values of functionalised starch-CNP (non irradiated sample) against all the pathogenic fungal strains were found to be 300µg/ml and irradiated sample (2 hrs) showed MIC 200 µg/ml. MIC results of the functionalised products against selected fungal strains are shown in table 4.

Table 4. MIC values of functionalised starch-CNP systems (nonirradiated sample and sample irradiated with visible light)

Systems	Fungal Strains	MIC values (nonirradiated)				MIC values (light irradiated 2hrs)			
		100 µg/ ml	200 µg/ ml	300 µg/ ml	400 µg/ ml	100 µg/ ml	200 µg/ ml	300 µg/ ml	400 µg/ ml
Functionally modified starch-CNP	A.niger	+	+	_	_	+	_	_	_
	A.fumigatus	+	+	_	_	+	_	_	_
	A.flavus	+	+	-	_	+	_	_	_
	Penicillium	+	+	+	_	+	_	_	_
	Mucor	+	+	+	_	+	_	_	_

+: growth, -: no growth

(b) Photoinduced antifungal activity of functionalised starch-CNP systems

The photoinduced antifungal effects of functionalised starch-CNP system were tested with Aspergillus niger, Aspergillus fumigates, Aspergillus flavus, Penicillium janthinellum and Mucor ramosissimus using well diffusion method. In this study the sample was irradiated with visible light by 0.5 hr, 1 hr, 2 hrs and 4 hrs. After incubation time (96 hrs) the zones of inhibition (in mm) were measured.

Results revealed that the functionally modified starch-CNP systems irradiated with visible light showed greater antifungal activity than the nonirradiated systems, in fact there was no appreciable change of inhibitory effect with different time intervals up to 2 hrs exposures. The strains susceptible to functionally modified CNP-starch complex exhibited greater activity in Aspergillus fumigates (28.00±1.00mm) on light exposure. The results of antifungal studies are summerised in table 5 and figure 16).

Table 5. Antifungal activities of functionalised starch-CNP systems (nonirradiated sample and sample irradiated with visible light)

	Functionally modified starch-CNP Zone of inhibition in mm at different time intervals				
	Zero hr	0.5 hr*	1 hr*	2 hrs*	4 hrs*
A.niger	24.33±0.471	24.66±0.577	25. 00±1.00	26.00±1.00	26.00±1.00
A.fumigatus	25.00±1.00	27.00±1.00	28.00±1.00	28.00±1.00	28.00±1.00
A.flavus	23.00±0.577	24.00±1.00	25.00±1.00	25.00±1.00	25.00±1.00
Penicillium	23.66±0.577	24.00±1.00	24.33±0.471	24.33±0.471	24.33±0.471
Mucor	22.00±1.00	24.66±0.577	25.66±0.577	25.66±0.577	25.66±0.577

Results are the means of three replications ± standard deviation

Zero hr- non irradiated sample

0.5 hr*- sample irradiated with visible light by 30 minitues

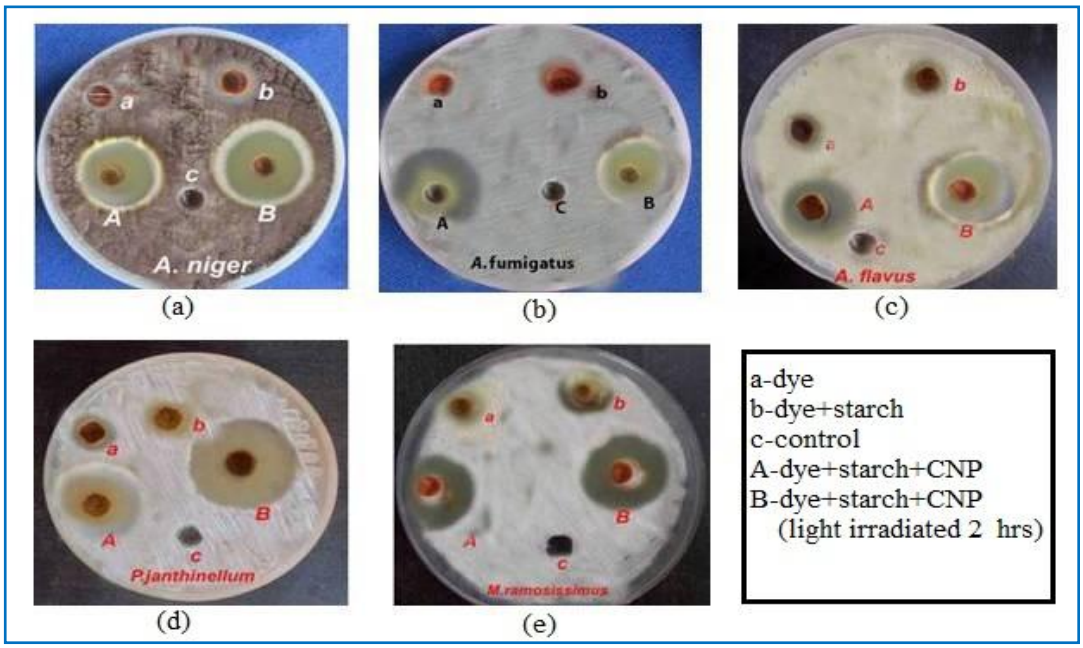

Figure 16. Antifungal activity of functionally modified starch-CNP against (a) A. niger (b) A. fumigates (c) A. flavus (d) P. janthinellum (e) M. ramosissimus.

Functionally modified starch acting as a capping agent which strongly prevent degradation and protect nanoparticles from aggregation and thereby stabilizing nanoparticles. Encapping of CNPs in the functionally modified core systems rendering photoresponsive materials with enhanced light absorption and excitation behaviour due to the effect of active carbon nanoparticles and photoactive groups. These systems have the ability to release simultaneously carbon nanoparticles and singlet oxygen (from the photosensiting dye molecules attached with the core systems) in the treated areas. The antifungal activity increases with increasing number of particles in the surface.

4. CONCLUSION

In this work we present a novel, effective and inexpensive nanosystem derived from natural sources by green methods, which is a highly efficient antifungal agent and can show biomedical applications. Attempts have been made to develop photostabilising nano systems. Binding chromophoric systems onto macromolecular systems systems enhance the thermal stability and light absorption and fluorescence emission properties. We have effectively synthesized photochromic group, {5-[4-(dimethylamino) benzylidene]-4-oxo-2-thioxo-1, 3-thiazolidin-3-yl} acetic acid and starch molecules functionally modified starch molecule and functionalised starch-CNP system. The products were characterized by UV-visible,

fluorescence, FT-IR, ^{1}HNMR spectroscopic methods and thermal analysis. Spectral studies showed that chromophoric system was successfully coupled into starch and CNP was effectively encapsulated in to the scaffolds or voids of these functionally modified systems. Functionally modified starch-CNP systems showed good thermal stability by TGA-DSC analysis. The light fastening studies of all the products found that stability of functionally modified starch-CNP systems was greatly enhanced and provides a new and novel photosensitive system with excellent light fastening properties. The antifungal activity of functionally modified starch-CNP systems was tested against selected pathogenic fungal strains such as Aspergillus niger, Aspergillus fumigates, Aspergillus flavus, Penicillium janthinellum, and Mucor ramosissimus. CNPs encapsulated in functionalised starch build up a highly aqueous soluble photoactive systems that are of great interest because of their noticeable photodynamic antifungal properties on light exposure. Functionally modified products induced with light exhibited good antifungal effects because of lower MIC values ($\geq$300µg/ml), notable inhibitiory zone (<24mm). This work explores the immense possibilities of our natural resources as biomedical and photodynamic agents if these are formulated into nanosized and nanostructured materials. The newly developed, inexpensive and biocompatible nanosystems were soluble in water and polar solvents, hence they can be utilized in biomedical applications, such as photodynamic therapy, photodynamic antimicrobial therapy and as a common modality for cancer and tumor treatment.

CONFLICT OF INTEREST

The authors report no conflicts of interest.

ACKNOWLEDGEMENT

The authors thank Department of Science and Technology (Ministry of Science and Technology), Govt. of India, New Delhi and University Grants Commission, New Delhi for financial support by awarding research projects (No.SR/S1/OC-24/2006, dtd.26.10.2006 and No.MRP(S)/ 13-14/ KLMG 027/ UGC-SWRO).

References

1. Ray, S. C.; Saha, A.; Jana, N. R.; Sarkar, R. J. Phys. Chem. C 2009, 113(43), 18546-18551.
2. Stepanidenko; Evgeniia A.; Elena V.; Ushakova, Anatoly V.; Fedorov.; Andrey L. Rogach. Nanomaterials 2021, 11, 364.
3. Yang, C.; Mamouni, J.; Tang, Y.; Yang, L. Langmuir 2010, 26(20), 16013-16019.
4. Garcez, A. S.; Nunez, S. C.; Hamblim, M. R.; Suzuki, H.; Ribeiro, M. S. J. Endod. 2020, 36(9), 1463-1466.
5. Schubauer-Berigan, M. K.; Dahm, M. M.; Yencken, M. S., J. Occup. Env. Med. 2011, 53, S62-S67.
6. Zhang, B. T.; Zheng, X.; Li, H. F.; Lin, J. M. Anal. Chim. Acta 2013, 784, 1-17.
7. Pyun, J. Angew. Chem. 2011, 50(1), 46-48.
8. Huang, J.; Deming, C. P.; Song, Y.; Kang, X.; Zhou, Z. Y.; Chen, S. Nanoscale 2012, 4(3), 1010-1015.
9. Varghese, S.; Kuriakose, S. Supramol. Chem. 2016, 28(3-4), 293-304.
10. Sharma, V. K.; McDonald, T. J.; Kim, H.; Garg, V. K. Adv. Colloid Interface Sci. 2015, 225, 229-240.
11. Rajesh, S.; Koshi, E.; Philip, K.; Mohan, A. J. Indian Soc. Periodontol. 2011, 15(4), 323.

12. Haag, R.; Stumbé, J. F.; Sunder, A.; Frey, H.; Hebel, A. Macromolecules 2000, 33(22), 8158-8166.
13. Vasileva, P.; Donkova, B.; Karadjova, I.; Dushkin, C. Colloids Surf. A 2011, 382(1), 203-210.
14. Raji, V.; Chakraborty, M.; Parikh, P. A. Part. Sci. Technol. 2012, 30(6), 565-577.
15. Zhu, S.; Zhang, J.; Qiao, C.; Tang, S.; Li, Y.; Yuan, W.; Gao, H. Chem. Commun. 2011, 47(24), 6858-6860.
16. Wang, L.; Su, D.; Zeng, L.; Liu, N.; Jiang, L.; Feng, X.; Kang, E. T. Dalton Trans. 2013, 42(37), 13642-13648.
17. George, C.; Kuriakose, S.; George, S.; Mathew, T. Supramol. Chem. 2011, 23(8), 593-597.
18. George, C.; Kuriakose, S.; Prakashkumar, B.; Mathew, T. Supramol. Chem. 2010, 22(9), 511-516.
19. Veerapandian, M.; Yun, K. Appl. Microbiol. Biotechnol. 2011, 90(5), 1655-1667.
20. Chandran, A.; Kuriakose, S.; Mathew, T. Int. J. Carbohydr. Chem. 2012, 2012, 1-8.
21. Dizaj, S. M.; Mennati, A.; Jafari, S.; Khezri, K.; Adibkia, K. Adv. Pharm.bull. 2015, 5(1), 19.
22. George, C.; Kuriakose, S.; Prakashkumar, B.; Mathew, T. Supramol. Chem. 2010, 22(9), 511-516.
23. Rettenbacher, A. S.; Elliott, B.; Hudson, J. S.; Amirkhanian, A.; Echegoyen, L. Chem. Eur. J. 2019, 12(2), 376-387.